Journal of Coastal Research	28	4	970–978	West Palm Beach, Florida	July 2012

TECHNICAL COMMUNICATIONS

Least Cost Path Extraction of Topographic Features for Storm Impact Scale Mapping

Eric Hardin[†], M. Onur Kurum[‡], Helena Mitasova[§], and Margery F. Overton[‡]

[†]Department of Physics
North Carolina State University
2401 Stinson Drive, Campus Box 8202
Raleigh, NC 27695, U.S.A.
ejhardi2@ncsu.edu

[‡]Department of Civil, Construction and Environmental Engineering
Campus Box 7908
North Carolina State University
Raleigh, NC 27695, U.S.A.

[§]Department of Marine, Earth and Atmospheric Sciences
North Carolina State University
Campus Box 8208
Raleigh, NC 27695, U.S.A.

ABSTRACT

Hardin, E.; Kurum, M.O.; Mitasova, H., and Overton, M.F., 2012. Least cost path extraction of topographic features for storm impact scale mapping. *Journal of Coastal Research,* 28(4), 970–978. West Palm Beach (Florida), ISSN 0749-0208.

A raster-based, spatially distributed implementation of the storm impact scale, designed to assess barrier island vulnerability, is presented. The two core topographic parameters of the scale, dune ridge and dune toe elevation, are extracted from a high-resolution, light detection and ranging (LIDAR)-derived digital elevation model (DEM). In addition, the beach slope, necessary to compute wave run-up, is extracted from the beach face. Innovative implementation of least cost path analysis and a physics-based model of an elastic sheet are used to map the dune ridge and dune toe. The robustness and efficiency of the topographic feature extraction method is demonstrated along 4 km of shoreline in Pea Island, Outer Banks, North Carolina.

ADDITIONAL INDEX WORDS: *Automated feature extraction, LIDAR, GRASS GIS, coastal dunes, barrier islands, erosion.*

INTRODUCTION

Coastal vulnerability to storm events depends on the storm characteristics and the continuously evolving, spatially varying beach and foredune topography (Morton, 2002; Wright, Swaye, and Coleman, 1970). Efforts to identify vulnerable locations have focused on characterizing the prestorm topographic features relative to storm parameters (*e.g.,* Garcia-Mora *et al*., 2001; Hallermeier and Rhodes, 1988; Jiménez *et al*., 2009; Jin and Overton, 2011; Judge, Overton, and Fisher, 2003; Sallenger, 2000; Stockdon, Sallenger, and Holman, 2007; Stockdon and Thompson, 2007a, 2007b). All of these efforts rely on topographic parameters (*e.g.,* dune ridge height, dune toe height, beach width, and beach slope) that are typically extracted from cross-shore profiles or digitized from three-dimensional surfaces. The need to perform regional scale analyses over potentially hundreds of profiles has driven the development of automated techniques for extraction of critical coastal features and estimation of their parameters.

One of the vulnerability assessment methods that requires dune and beach parameters is the storm impact scale (Sallenger, 2000). It specifies four distinct erosion regimes that can occur during storm events. These regimes are defined by the elevations of the prestorm dune ridge D_{High} and the dune toe D_{Low} relative to the storm surge elevation with and without run-up, R_{High} and R_{Low}, respectively. Wave run-up is typically estimated using the 2% exceedance levels and is a function of beach slope, tan β, and the deep water wave height and period. The four distinct erosion regimes are as follows:

- The *swash* regime occurs when $R_{\mathrm{High}} < D_{\mathrm{Low}}$ and is characterized by beach erosion and a likely poststorm recovery.
- The *collision* regime occurs when $D_{\mathrm{Low}} < R_{\mathrm{High}} < D_{\mathrm{High}}$, leading to dune erosion, with eroded sand unlikely to be redeposited back onto the dune after the storm.
- The *overwash* regime occurs when $R_{\mathrm{High}} > D_{\mathrm{High}}$ and is characterized by severe dune erosion and inland transport of sediment.
- Finally, the *inundation* regime occurs when $R_{\mathrm{Low}} > D_{\mathrm{High}}$.

The inundation of a barrier island can flatten dunes, cause massive inland and offshore transport of sediment, and lead to barrier island breaching.

DOI: 10.2112/JCOASTRES-D-11-00126.1 received 11 July 2011; accepted in revision 1 December 2011.
Published Pre-print online 16 March 2012.

Implementation of the storm impact scale requires both the topographic parameters and the storm characteristics. The dune ridge (D_{High}), the dune toe (D_{Low}), and the beach slope can be extracted from the topographic data. Storm characteristics are obtained poststorm from offshore wave and tide gauges or can be simulated either in forecast or hindcast mode from numerical storm surge and wave models. The relationship of the beach and dune topography together with the specified storm characteristics determines the likely outcome of the poststorm profile. In this way, the site-specific coastal vulnerability is inferred.

Profile-based, automated extraction procedures have been developed for the storm impact scale. Elko *et al*. (2002) proposed a geographic information system (GIS)-based, semi-automated procedure for measuring the elevations of dune toe and dune ridge. First, a digital elevation model (DEM) is interpolated from topographic light detection and ranging (LIDAR) using Delaunay triangulation. Operators then use the DEM to coarsely digitize the dune ridge and the dune toe. The digitized dune ridge is then refined using a GIS-based algorithm, which searches along profiles, placed at DEM resolution, for the highest elevation in the vicinity of the digitized line. After the dune ridge has been refined, it is inspected to ensure that the extracted dune ridge is continuous and no high-elevation feature such as a house or utility wire has been mistakenly selected. Similarly, the dune toe is coarsely digitized along the highest curvature, refined using an analogous GIS-based algorithm, and checked for continuity to ensure that the dune toe was selected as opposed to a small-scale topographic anomaly. Owing to the subjectivity of human digitization, the procedure requires that five operators repeat the analysis independently to estimate the accuracy. Recently, Stockdon, Doran, and Sallenger (2009) proposed an automated profile-based procedure for estimating the dune toe and dune ridge elevation. First, beach profiles are generated by interpolating and smoothing LIDAR data within a user-defined beach width. Then, the first elevation peak landward of the shoreline is located by identifying the location where the profile slope changes sign. The method is highly dependent on the smoothing parameter. If the smoothing parameter is too small, noise in the LIDAR will cause the slope of the profile to change sign many times between the shoreline and foredune. On the other hand, a smoothing parameter that is too large can smooth away salient features like an incipient foredune and bias the dune ridge toward a lower elevation.

In this paper, we present a spatially distributed, raster-based approach for extracting the dune ridge, dune toe, and the beach slope in a GIS environment through the innovative use of the least cost path analysis and a physics-based model of an elastic sheet. To demonstrate the application of the presented automated analysis, the extracted features are used for the GIS-based computation of the storm impact scale. The GIS-based implementation enables the storm impact scale to be computed and visualized at the high resolution of the input DEM.

METHODS

To improve the efficiency of the profile-based storm impact scale computation, we have developed a GIS-based, highly automated feature extraction procedure. The efficiency and robustness of the procedure is achieved by employing the least cost path analysis for extraction of D_{High} and D_{Low} from a LIDAR-derived DEM. Least cost path analysis is a GIS technique used to find an optimal path connecting two geographic points. The technique can be applied to a number of problems including military operations planning (Lee and Stucky, 1998), stream extraction from DEMs (Metz, Mitasova, and Harmon, 2011), and wildlife migration modeling (Walker and Craighead, 1997). The cost of a path is calculated according to a cost function where the cost can be time, energy, or any other quantitative measure. In our case, the cost is based on the elevation surface geometry and the optimal path is intended to approximate the location of the dune ridge (Mitasova *et al*., 2011).

The least cost path analysis approach to dune ridge and dune toe extraction offers possible advantages. First, the method is easy to implement because it employs two standard GIS algorithms: cumulative cost surface generation and least cost path tracing (Neteler and Mitasova, 2008; Ch. 5, pp. 135–138). Second, the least cost path method only requires a starting and an ending point from the user. These two points are located along opposite ends of the studied dune ridge and can be manually digitized or selected using a profile-based method as in Stockdon, Doran, and Sallenger (2009).

Third, cost surface analysis is a spatially distributed approach to linear feature extraction because it approximates a continuous dune ridge according to the cumulative cost surface, which is generated using the entire DEM. This makes the method robust to localized topographic extremes like high-elevation houses or high-curvature terrain indents. More traditional profile-based feature extraction methods that identify the features as a maximum value along a profile are susceptible to inaccurate selections because the profiles are treated independently of each other (Hardin, Mitasova, and Overton, 2010).

Dune Ridge Extraction, D_{High}

The least cost path approach to dune ridge extraction requires a suitable quantitative definition of the dune ridge so that a cost surface can be generated and the least cost path can be found. There are a number of conditions that the cost function must satisfy. First, the cost function must be an inverse function of elevation because the dune ridge is at a local elevation maximum and the paths that pass below the dune ridge should have high cumulative costs. Second, the least cost path is found based on the cost of passing through a grid cell and the traveled distance, and to account for the complexity of dune ridges, the cost of a slightly shorter, lower elevation path should be greater than a slightly longer, higher elevation path. Third, the cost function should be continuous everywhere, unlike z^{-1} and other power functions, which can satisfy the above two conditions but are discontinuous at $z = 0$. Finally, the cost function should be positive everywhere. This means that the cost should approach zero as elevation increases as opposed to approaching negative infinity. The cost function that was found to fulfill the above stated conditions was defined as

$$J_{ij} = e^{-\alpha z_{ij}} \tag{1}$$

where J_{ij} is the dimensionless cost of traversing the raster cell (i,j), z_{ij} [m] is the DEM elevation, and α [m^{-1}] is a tunable parameter. The dune ridge is then extracted by generating the cumulative cost surface and finding the path with the least cumulative cost:

$$J_{\text{tot}} = \min_{n} \sum_{n}^{N} J_{i_n j_n} \tag{2}$$

where J_{tot} is the cumulative cost, n indexes over the cells in the path, N is the number of cells in a path, and the starting and ending points, (i_0, j_0) and (i_N, j_N), are fixed at the ends of the studied dune ridge. The cost surface described by Equation (1) can be generated in a GIS using map algebra, and the least cost path described by Equation (2) can be calculated using standard cumulative cost surface generation and least cost path routing tools.

Dune Toe Extraction, D_{Low}

The dune toe is qualitatively regarded as the location where the beach meets the coastal foredune. It is often identified along a cross-shore beach profile as the location with the greatest change in slope (profile curvature maximum) or where shallow sloping terrain on the beach meets steep foredune terrain (Burroughs and Tebbens, 2008; Elko *et al.*, 2002; Stockdon, Sallenger, and Holman, 2007; Stockdon and Thompson, 2007a,b). Estimating the curvature requires computation of second-order derivatives of an intrinsically noisy surface, which makes the curvature-based dune toe extraction methods highly dependent on resolution and smoothing parameters.

Alternatively, the dune toe can be identified as the location where an elevation profile is most separated from a line connecting the dune ridge and shoreline (Mitasova *et al.*, 2011). A continuous dune toe can be extracted by implementing this conceptualization in two dimensions, where the beach profile becomes the terrain surface and the line connecting the dune ridge and shoreline becomes a tightly stretched elastic sheet with boundary conditions at the dune ridge and shoreline (Figure 1a). Further, instead of approximating the dune toe as the point where the elevation profile is most deviated from a line connecting the dune ridge and shoreline, the path of greatest deviation between the terrain surface and the elastic sheet (Figure 1b) approximates the continuous dune toe (Figure 1c).

The elastic sheet is modeled as an array of springs with nodes located at each raster cell (Mitasova *et al.*, 2011), which is a basic model for a deformable cloth that is well established in computer graphics literature (Breen, House, and Getto, 1992; Provot, 1995). The nodes between the shoreline and dune ridge move vertically but do not move horizontally because of equilibrium resulting from the uniform raster spacing. The nodes at the ends of the sheet are fixed to the shoreline and the dune ridge. The motion of each node is determined by a spring force (which depends on its elevation relative to the elevation of neighboring nodes) and a mechanical damping force (which depends on its velocity relative to the velocity of its neighbors). The spring force provides the tension needed to tightly stretch the sheet between the shoreline and the dune ridge, and the mechanical damping dissipates energy to ensure that the sheet comes to equilibrium. The motion of a node in raster cell i, j is described by

$$\ddot{z}_{i,j} + 2\zeta\omega_0\Delta^{i,j}\dot{z}_{i,j} + \omega_0^2\Delta^{i,j}z_{i,j} = 0 \tag{3}$$

where $z_{i,j}$ [m] is the elevation of the node; t [s] is time; ω_0 [rad/s^2] is the angular frequency of oscillation, which has been set to one for simplicity; and ζ is the dimensionless damping ratio, which has been set to one in order to critically damp the motion of the node to ensure that it approaches equilibrium as quickly as possible. Dots indicate time derivatives, and $\Delta^{i,j}$ is the summation of differences with nearest neighbor values, *e.g.,*

$$\begin{aligned}\Delta^{i,j}z_{i,j} = {} & \left(z_{i,j} - z_{i+1,j}\right) + \left(z_{i,j} - z_{i-1,j}\right) \\ & + \left(z_{i,j} - z_{i,j+1}\right) + \left(z_{i,j} - z_{i,j-1}\right).\end{aligned} \tag{4}$$

Equation (3) can be easily solved by first writing it as a system of two, first-order ordinary differential equations: let

$$q_1 = z \tag{5}$$

and

$$q_2 = \dot{z}. \tag{6}$$

It follows that

$$\dot{q}_1 = q_2 \tag{7}$$

and

$$\dot{q}_2 = -2\zeta\omega_0 q_2 - \omega_0^2 q_1. \tag{8}$$

Equations (7) and (8) can be solved using standard numerical techniques like Runge-Kutta. Nodes were given the initial conditions

$$z(t = 0) = 0 \tag{9}$$

and

$$\dot{z}(t)|_{t=0} = 0. \tag{10}$$

Once the elevation of the elastic sheet is solved, the elevations of the sheet and the terrain surface are differenced to produce a raster map that represents the deviation between the two surfaces, $D_{i,j}$ (Figure 1b). Finally, the cost surface is derived using Equation (1) where $z_{i,j}$ has been replaced by the difference between the DEM and the sheet, $D_{i,j}$, and the dune toe is extracted as the least cost path using Equation (2) (Figure 1c).

Beach Slope Approximation

Once the dune toe is extracted, the beach slope tan β can be estimated, although slope can be computed at any point on a profile or location on a DEM. Stockdon, Sallenger, and Holman (2007) proposed that mean beach slope, defined as the slope of a cross-shore line connecting dune toe and shoreline, was the most robust and relevant slope to the wave run-up model. The shoreline is identified using a contour or constant elevation approach, *e.g.,* mean high water. To approximate the mean

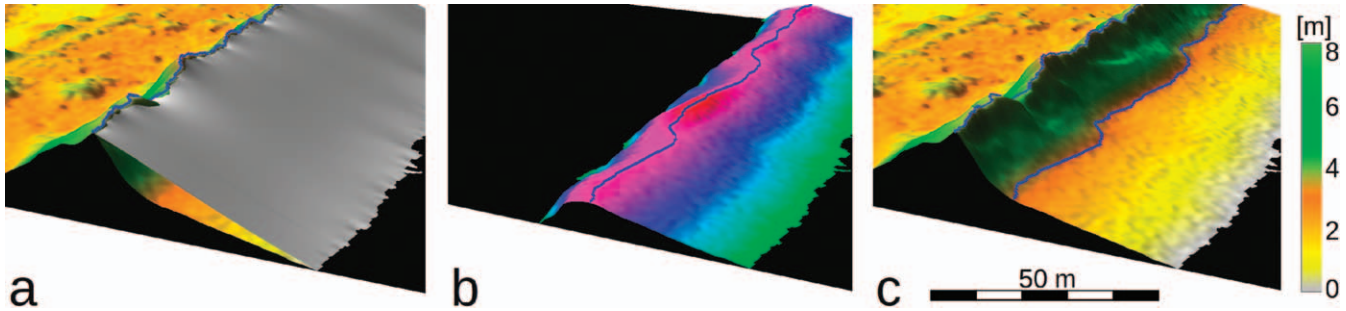

Figure 1. Illustration of the dune toe extraction method: (a) the elevation of an elastic sheet with boundary conditions at the shoreline and the dune ridge is computed; (b) the elevation of the sheet and terrain surfaces are differenced to produce a deviation surface, and the path of the highest deviation representing the dune toe line is extracted; (c) the dune toe is overlaid on the terrain surface. The surfaces are rendered with three times vertical exaggeration.

beach slope in two dimensions, an elastic sheet is again simulated but with boundary conditions at the shoreline and the dune toe. Then, a grid is aligned with the shoreline and each shore-perpendicular row is assigned the mean slope of the elastic sheet that approximates the beach. Finally, a north-aligned raster map representing beach slope is computed from the shore-aligned beach slope raster map using a nearest neighbor approach. The shore-aligned grid is used because the wave run-up model inherently models run-up in the shore-perpendicular direction and because the elevation of wave run-up on the dune face (in the case of the collision and overwash regimes) is dependent on the beach slope.

In practice, any beach slope estimate that is considered to be most relevant could be used to calculate R_{Low} and R_{High}. It should be stressed that the main contribution of this work is the dune features extraction and implementation of a storm impact model in two dimensions within a GIS framework and not in the particular wave run-up model used.

Run-Up, R_{Low} and R_{High}

Once beach slope is obtained, storm surge and wave characteristics can be used to compute raster surfaces representing R_{Low} and R_{High}. Run-up is calculated in the beach area and extended in the shore-perpendicular direction to assess erosion vulnerability on the dunes. Once R_{Low} and R_{High} are computed, the erosion vulnerability regime can be visualized by displaying the raster surfaces representing R_{Low} and R_{High} along with the terrain surface (Figure 2).

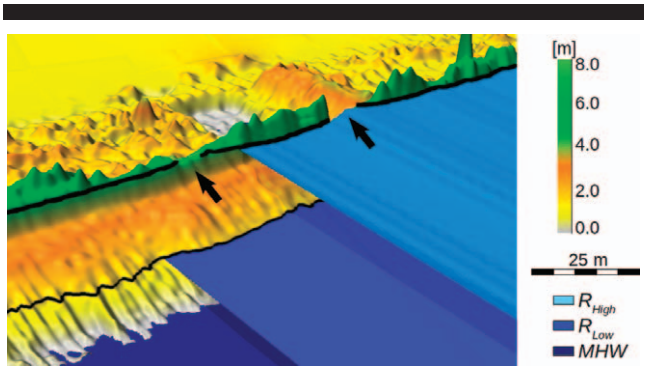

Figure 2. Relation between the terrain surface and the surfaces representing R_{High}, R_{Low}, and the mean high water level (MHW) used to compute the storm impact scale. The locations marked with black arrows are vulnerable to overwash, whereas other locations are vulnerable to the collision regime.

The wave run-up model used here is the same used by Sallenger (2000), which was first determined by Holman (1986). However, any run-up model can be used to compute vulnerability. Also, it should be emphasized that any georeferenced output from a numerical grid used to calculate storm surge and wave characteristics can be used to compute raster surfaces representing R_{Low} and R_{High} using standard GIS tools and then used to implement a raster-based storm impact scale.

Sensitivity Analysis

Elko *et al*. (2002) quantified procedural error in D_{High} measurements arising from the subjectivity of human digitization by comparing results from multiple operators. Error was quantified by designating one operator as the "standard operator" and then measuring vertical differences between measurements made by the standard operator and the other operators. The average root-mean-squared vertical error using the method of Elko *et al*. (2002) was 0.05 m. Topographically similar dunes were used in our application (Elko *et al*., 2002), which is favorable for quantitative comparison. However, within the least cost path approach the DEM uncertainty as opposed to human subjectivity is considered the major source of uncertainty in the dune ridge extraction.

To evaluate the sensitivity of extracted ridge positions to DEM uncertainty, a Monte Carlo method was used. First, a predictive error map of the LIDAR-derived DEM was estimated using a cross-validation procedure (Neteler and Mitasova, 2008, Ch. 6, pp. 243–244). With the predictive error map, 1000 instances of the terrain surface were generated by adding Gaussian noise to the original DEM with zero mean and standard deviation equal to the predictive error. Dune ridges were then extracted from each of the 1000 DEM instances. To measure uncertainty in a way that was consistent with Elko *et al*. (2002), the median dune ridge extraction was used in place of the "standard operator" extraction.

APPLICATION

To demonstrate the effectiveness and robustness of the presented approach, the U.S. Geological Survey (USGS) storm impact scale due to Hurricane Isabel (landfall in 2003) was computed for a 4-km section of the Outer Banks, North Carolina. The study site is located in the Pea Island National Wildlife Refuge (PINWR) and is also known as Old Sandbag Area. The PINWR is undeveloped with the exception of highway NC12 and PINWR facilities. A dune system exists between the shoreline and the highway. The dunes were constructed in the 1930s by the National Park Service to offer protection against coastal hazards. The dune system was maintained into the 1970s when maintenance was ceased (Birkemeier, Dolan, and Fisher, 1984; DeKimpe, Dolan, and Hayden, 1991). Owing to frequent overwashing and storm-induced damage to NC12, the area is recognized by the North Carolina Department of Transportation as one of five "NC12 Hotspots" along the Outer Banks (Stone, Overton, and Fisher, 1991).

Input Data

The LIDAR point data used to interpolate the high-resolution DEM were collected as part of the National Aeronautics and Space Administration (NASA)/USGS Experimental Advanced Airborne Research LIDAR program. The point data were transformed to the state plane coordinate system relative to mean high water (MHW) in units of meters. The transformation of data to MHW was performed using the vertical datum transformation tool (VDatum; Parker *et al.*, 2003). On flat terrain, the root-mean-squared vertical accuracy of the data is approximately 15 cm, and the horizontal accuracy is better than 2 m. The LIDAR data were interpolated to generate a 0.5-m resolution DEM using regularized spline with tension while simultaneously smoothing noise (Mitasova, Mitas, and Harmon, 2005).

After the DEM was generated, the location of the shoreline was approximated by the MHW contour, and the dune ridge and dune toe were extracted using the least cost path approach. The LIDAR was first return and contained buildings and vegetation. There is no vegetation or buildings on the dune ridge in this area, and tall features (such as buildings and tall vegetation) that are spatially small and located away from the dune ridge do not influence the dune ridge extraction. Therefore, it was unnecessary to limit the extraction area to within a threshold beach width, elevation, or slope value prior to extracting the dune ridge.

The water level used in the application was generated from an ADCIRC (Luettich, Westerink, and Scheffner, 1992) simulation of the conditions during Hurricane Isabel. Results from the ADCIRC grid (which had a median grid element size of 148 m) were converted to raster format at half meter resolution using a nearest neighbor Voronoi polygon approach. A neighborhood averaging operation was applied to the resultant raster to ensure a smooth surface.

Values for deep water wave height and wave period were downloaded from the website of the U.S. Army Corps of Engineers Field Research Facility (FRF), located in Duck, North Carolina. The wave period was used to compute the deep water wave length using the linear dispersion relation for deep water (Sorensen, 1993). Values for deep water wave length and wave height were used to compute surfaces representing R_{Low} and R_{High} from the surface representing maximum water elevation (Figure 2).

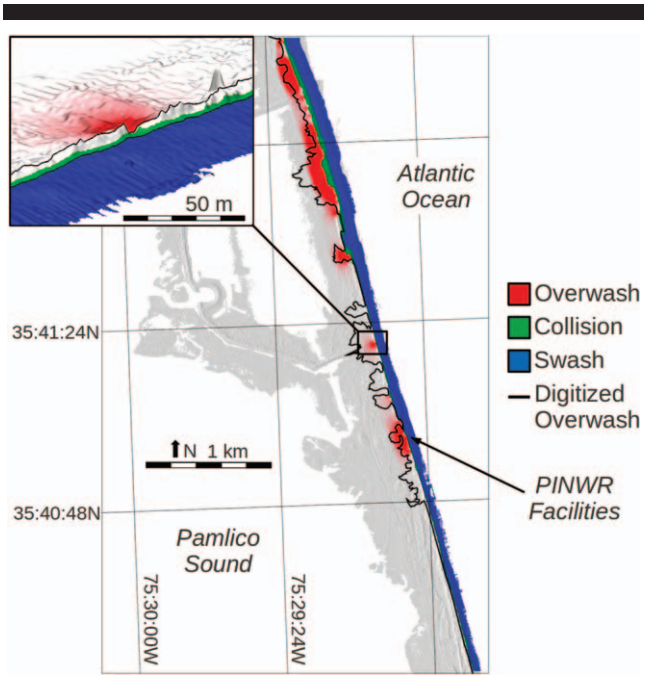

Figure 3. Location of the study area with the erosion regimes, as predicted by the raster implementation of the storm impact scale, overlaid over terrain. Overwash fans digitized from the post-Isabel aerial photography are shown as black lines. The inset (rendered with three times vertical exaggeration) shows a degraded dune section where overwash was predicted. Vulnerability regimes are displayed between the features that define them (*i.e.,* the swash regime between the shoreline and dune toe, collision regime between the dune toe and ridge, and overwash is displayed landward of the dune ridge).

Storm Impact Scale Map

The area was initially screened for the maximum storm impact (*i.e.,* inundation) by using map algebra to determine whether and where R_{Low} was greater than the dune ridge elevation. In this case, no area was subject to inundation. Second, the DEM was compared with R_{High}, and each raster cell in the DEM that was lower than R_{High} was determined to be vulnerable to storm impact. For purposes of display, the map is color coded relative to the storm impact regimes of overwash, collision, and swash. The particular vulnerability regime displayed on each raster cell depended on the position of the cell relative to the features that define the regime (*e.g.,* raster cells located between the dune toe and dune ridge that were below R_{High} were displayed as being vulnerable to the collision regime because the collision regime is defined by the condition $D_{Low} < R_{High} < D_{High}$). At any location along the shoreline, the storm impact scale characterizes that location with the highest

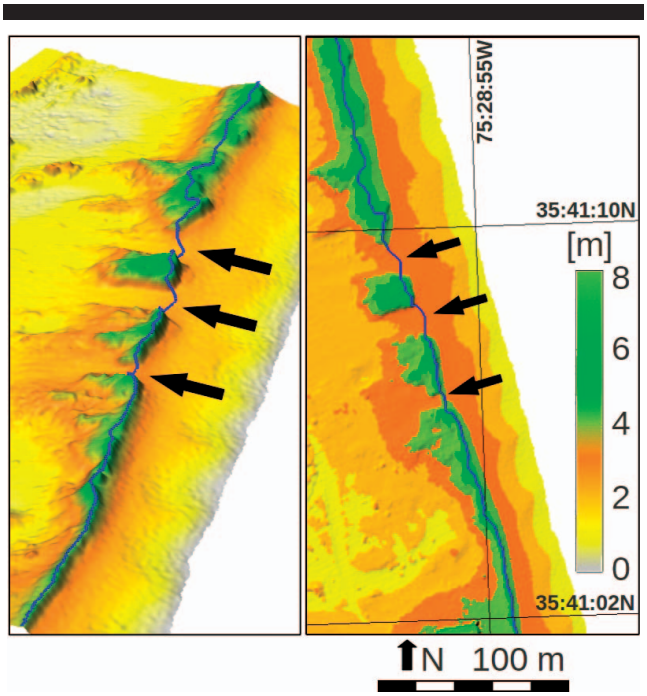

Figure 4. Example of a degraded dune (marked with black arrows) where the location of the dune ridge is uncertain and the least cost path represents an optimal high-elevation path connecting endpoints of the well-defined dune ridge. The geospatial information provided by the least cost path in this case is important because the degraded areas are likely to be vulnerable because of their low elevation.

vulnerability mapped; however, in the raster implementation of the storm impact scale the regime breakpoints are provided to visualize the transitioning vulnerability across the beach and dune face.

Figure 3 consists of a plan view of the study area with the three storm-impact regimes due to Hurricane Isabel mapped as described above. Further, the landward extent of the washover deposits digitized from poststorm orthophotos is provided for context in the overwash areas. The inset in Figure 3 shows a three-dimensional view of an area of low-elevation dune approximately 10 m in length where the raster implementation of the storm impact scale predicted that the terrain landward of this low spot was vulnerable to overwash and neighboring dunes were vulnerable to collision. Over the entire study area, 26% or 1.2 km of the dune ridge length was predicted to be vulnerable to overwash, 73% to collision, and 1% to swash only.

Sensitivity of the Extracted Dune Ridge to DEM uncertainty

The mean absolute predictive error of the LIDAR-derived DEM, estimated by the cross-validation procedure, was 0.010 m with a standard deviation of 0.012 m. Error values were larger on the dune due to the steep slopes and high curvatures. The average root-mean-squared vertical error of the dune ridges extracted from the 1000 DEM instances generated by Monte Carlo method was 0.02 m, where the dune ridge with the median horizontal position was used in place of the "standard operator" extraction. Additionally, the horizontal envelope containing all of the extracted dune ridges had a mean width of 1.30 m with a standard deviation of 0.42 m, and 95% of the envelope had a width of less than 2.00 m. The error of the dune ridge extraction method is within LIDAR data uncertainty, in agreement with the method presented by Elko *et al*. (2002). However, by ensuring a continuous line extraction and by removing reliance on local topographic maxima, the least cost path approach is more robust to topographic extremes that are close to the dune ridge (such as buildings and tall vegetation). This robustness allows for a higher level of automation.

The Role of the Cost Function Parameter α

In addition to the DEM uncertainty, the location of the extracted dune ridge is also influenced by the dune geometry. In locations with degraded dunes that do not have a continuous well-developed dune ridge (Figure 4), the least cost path approach extracts an optimized high-elevation path as an approximation of the dune ridge. In this way, the ridge elevations can be estimated even in areas with degraded dunes where the vulnerability assessment is particularly important.

The complexity of the least cost path line geometry can be adjusted using the tunable parameter, α, which has been set empirically to $\alpha = \ln 10$ for our specific conditions. High values of α yield more complex approximations, whereas lower values of α yield more linear approximations (Figure 5). Values for α can be optimized for a given application using a representative sample of the dune ridge where a highly accurate location of the dune ridge and toe is available (for example obtained by manual digitization or from field survey). The optimized α will also depend on the scale of the process being modeled.

Evaluation of Performance

To evaluate the predictive capabilities of the storm impact scale, the predicted vulnerability to the overwash regime was compared with outlines of overwash fans that were digitized from post-Isabel aerial photography (Figure 3). It should be noted that the areas indicating overwash vulnerability in the storm impact scale map are nonquantitative illustrations. Their size is only determined by the length of dune that is predicted to be vulnerable to overwash. Therefore, only the location and not the extent of red areas should be expected to coincide with the outlined overwash fans.

Figure 3 shows that the predicted overwash vulnerability agreed well with the observed overwash occurrence, particularly in the northern section of the study area. The storm impact scale did not predict overwash where it did not occur; however, it failed to predict overwash in three locations where it did occur. While the estimation of parameters may have contributed to this, it is important to point out that the storm impact scale does not take into account erosion processes that take place during the storm. For example, in the overwash area illustrated in the inset of Figure 3, erosion processes occurring both on the dune face and laterally within the initial low point of the dune ridge could cause a loss of dune material to a larger spatial extent than is mapped by the storm-impact scale.

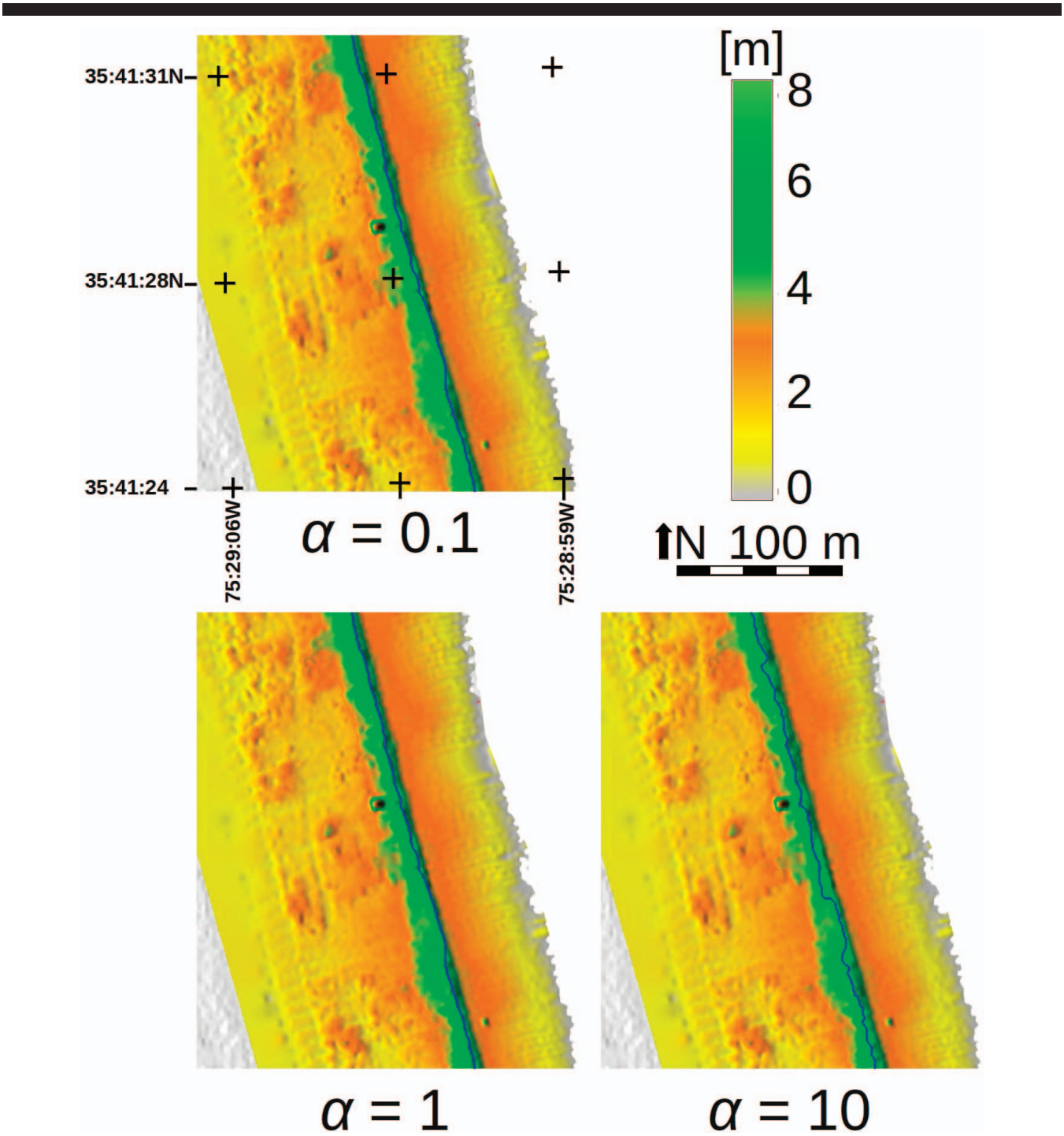

Figure 5. Three extracted dune ridges approximated using different values of α, illustrating the scale of topographic detail controlled by this parameter.

Likewise in areas that are not mapped as overwash areas ($R_{High} < D_{High}$), dune face erosion could cause an undermining and loss of material within the collision zone leading to the subsequent collapse of the dune ridge, essentially lowering D_{High} during the storm and allowing overwash.

The dune ridge extraction at 0.5-m resolution along 4 km of beach was performed on a personal computer using Geographic Resources Analysis Support System (GRASS GIS; Neteler and Mitasova, 2008, http://grass.osgeo.org/). The dune ridge extraction (*i.e.,* generation of the cost surface, cumulative cost surface, and least cost path) took approximately 1.5 minutes. The elevation of the elastic sheet (described by Eq. 7) was solved using second-order Runge-Kutta with an adaptive time step, which was implemented using the Java programming

language. The simulation of the elastic sheet completed in 1 hour 20 minutes. It is likely that the computational time could be considerably reduced if more emphasis were placed on implementation of the sheet model.

CONCLUSIONS

In this paper, we presented a least cost path approach to the extractions of the dune ridge and dune toe from high-resolution, LIDAR-based DEMs. The elevations of these two features are essential parameters in many coastal vulnerability models, and by estimating these elevations along continuous, least cost paths, the existing profile-based vulnerability models can be efficiently implemented within a raster-based GIS framework. A Monte Carlo experiment demonstrated robustness of the approach to topographic anomalies and uncertainty in DEM.

To demonstrate the effectiveness of the methodology, the USGS storm impact scale was implemented within a GIS and applied to assess vulnerability of a 4-km section of the Outer Banks of North Carolina due to Hurricane Isabel. In addition to providing the advantages and efficiencies of automated analysis and mapping, these tools provide high-resolution information that can be mapped over a continuous topographic surface as opposed to cross-sectional profiles.

ACKNOWLEDGMENTS

The authors would like to acknowledge the Field Research Facility, Field Data Collections and Analysis Branch, U.S. Army Corps of Engineers, Duck, North Carolina, for data on wave conditions during Hurricane Isabel. The authors would also like to acknowledge NASA and the USGS, who were responsible for the LIDAR data collection prior to Hurricane Isabel, as well as Dr. Asbury Sallenger for providing the data. We are grateful to UNC's Renaissance Computing Institute and Dr. Brian Blanton for advice on high-performance computing and ADCIRC modeling. This material is based upon work partially supported by the U.S. Department of Homeland Security under Award Number 2008-ST-061-ND0001 and by the Army Research Office.

DISCLAIMER

The views and conclusions contained in this document are those of the authors and should not be interpreted as necessarily representing the official policies, either expressed or implied, of the U.S. Department of Homeland Security.

LITERATURE CITED

Birkemeier, W.; Dolan, R., and Fisher, N., 1984. The evolution of a barrier island: 1930–1980. *Journal of the American Shore and Beach Preservation Association*, 52(2), 2–12.

Breen, D.E.; House, D.H., and Getto, P.H., 1992. A physically-based particle model of woven cloth. *The Visual Computer*. 8(5–6), 264–277. DOI: 10.1007/BF01897114.

Burroughs, S. and Tebbens, S., 2008. Dune retreat and shoreline change on the Outer Banks of North Carolina. *Journal of Coastal Research*, 24, 104–112.

DeKimpe, N.M.; Dolan, R., and Hayden, B.P., 1991. Predicted dune recession on the Outer Banks of North Carolina, USA. *Journal of Coastal Research*, 7(2), 451–463.

Elko, N.A.; Sallenger, A.H.; Guy, K.; Stockdon, H.F., and Morgan, K.L.M., 2002. Barrier Island Elevations Relevant to Potential Storm Impacts: 1. Techniques. U.S. Geological Survey, Center for Coastal Geology.

Garcia-Mora, M.R.; Gallego-Fernandez, J.B.; Williams, A.T., and Garcia-Novo, F., 2001. A coastal dune vulnerability classification. A case study of the SW Iberian Peninsula. *Journal of Coastal Research*, 17(4), 802–811.

Hallermeier, R.J. and Rhodes P.E., 1988. Generic treatment of dune erosion for 100-year event. *In: Proceedings of the 21st International Conference on Coastal Engineering* (Coata del Sol-Malaga, Spain, ASCE), pp. 1121–1197.

Hardin, E.; Mitasova, H., and Overton, M., 2010. Sensitivity analysis of dune height measurements along cross-shore profiles using a novel method for dune ridge extraction. *American Geophysical Union, Fall Meeting 2010*, abstract EP33B-0765.

Holman, R., 1986. Extreme value statistics for wave run-up on a natural beach. *Coastal Engineering*, 9(6), 527–544. DOI: 10.1016/0378-3839(86)90002-5.

Jiménez, J.A.; Ciavola, P.; Balouin, Y.; Armaroli, C.; Bosom, E., and Gervais, M., 2009. Geomorphic coastal vulnerability to storms in microtidal fetch-limited environments: Application to NW Mediterranean and N Adriatic Seas. *In:* da Silva (ed.), *Proceedings of the 10th International Coastal Symposium,* Journal of Coastal Research, Special Issue, No. 56, pp. 1641–1645.

Jin, Q. and Overton, M., 2011. Quantitative analysis of coastal dune erosion based on geomorphology features and model simulation. *Proceedings of the Coastal Sediments 2011, Miami Florida*, 1825–1840.

Judge, E.K.; Overton, M.F., and Fisher, J.S., 2003. Vulnerability indicators for coastal dunes. *Journal of Waterway, Port, Coastal, and Ocean Engineering*, 129(6), 270–278. DOI: 10.1061/(ASCE)0733-950X(2003)129:6(270).

Lee, J. and Stucky, D., 1998. On applying viewshed analysis for determining least-cost paths on digital elevation models. *International Journal of Geographical Information Science*, 12(8), 891–905.

Luettich, Jr., R.; Westerink, J., and Scheffner, N., 1992. ADCIRC: An Advanced Three- Dimensional Circulation Model for Shelves, Coasts, and Estuaries. Report 1. Theory and Methodology of ADCIRC-2DDI and ADCIRC-3DL. Technical Report ADA261608. Vicksburg, Mississippi: Coastal Engineering Research Center.

Metz, M.; Mitasova, H., and Harmon, R.S., 2011. Efficient extraction of drainage networks from massive, radar-based elevation models with least cost path search. *Hydrology and Earth System Sciences*, 15(2), 667–678. DOI: 10.5194/hess-15-667-2011.

Mitasova H.; Hardin E.; Starek, M.J.; Harmon R.S., and Overton, M.F., 2011. Landscape dynamics from LiDAR data time series. *In:* Hengl, T.; Evans, I.S.; Wilson, J.P.; and Gould, M. (eds.), *Geomorphometry 2011* (Redlands, California), pp. 3–6. http://geomorphometry.org/Mitasova2011

Mitasova, H.; Mitas, L., and Harmon, R., 2005. Simultaneous spline approximation and topographic analysis for lidar elevation data in open-source GIS. *IEEE Geoscience and Remote Sensing Letters*, 2:375–379. DOI: 10.1109/LGRS.2005.848533.

Morton, R.A., 2002. Factors controlling storm impacts on coastal barriers and beaches: A preliminary basis for near real-time forecasting. *Journal of Coastal Research,* 18(3), 486–501.

Neteler, M. and Mitasova, H., 2008. *Open Source GIS: A GRASS GIS Approach*, third edition. New York: Springer.

Parker, B.; Milbert, D.; Hess, K., and Gill, S., 2003. National VDatum—The implementation of a national vertical datum transformation database. *In: Proceedings of the U.S. Hydro 2003 Conference, March 24–27, 2003*. (Biloxi, Mississippi), pp. 24–27.

Provot, X., 1995. Deformation constraints in a mass-spring model to describe rigid cloth behaviour. *In: Proceedings of Graphics Interface 95*, (Quebec, Canada), pp. 147–154.

Sallenger, A., 2000. Storm impact scale for barrier island. *Journal of Coastal Research*, 16(3), 890–895.

Sorensen, R., 1993. *Basic Wave Mechanics for Coastal and Ocean Engineers*. New York: Wiley- Interscience.

Stockdon, H.; Doran, K., and Sallenger, A., 2009. Extraction of lidar-based dune-crest elevations for use in examining vulnerability of beaches to inundation during hurricanes. *In:* Stockden et al. (2009). (eds.), *Proceedings of the 12th International Coastal Symposiu*. Journal of Coastal Research, Special Issue, No. 53, pp. 59–65.

Stockdon, H.; Sallenger, A., and Holman, R., 2007. A simple model for the spatially-variable coastal response to hurricanes. *Marine Geology*, 238, 1–20. DOI: 10.1016/j.margeo.2006.11.004.

Stockdon, H. and Thompson, D., 2007a. Vulnerability of National Park Service Beaches to Inundation During a Direct Hurricane Landfall: Cape Lookout National Seashore. U.S. Geological Survey Open-File Report 2007-1376, 8 p.

Stockdon, H. and Thompson, D., 2007b. Vulnerability of National Park Service Beaches to Inundation During a Direct Hurricane Landfall: Fire Island National Seashore. U.S. Geological Survey Open-File Report 2007-1389, 8 p.

Stone, J.; Overton, M.F., and Fisher, J., 1991. Options for North Carolina Coastal Highways Vulnerable to Long Term Erosion. Report prepared for the North Carolina Department of Transportation and the U.S. Department of Transportation Federal Highway Administration.

Walker, R. and Craighead, L., 1997. Analyzing wildlife movement corridors in Montana using GIS. *ESRI User Conference* (San Diego, CA, July 1997), pp. 8–11.

Wright, L.D.; Swaye, J.M., and Coleman, F.J., 1970. Effects of Hurricane Camille on the landscape of the Brenton-Chandeleur island chain and the eastern portion of the lower Mississippi delta. Baton Rouge: Louisiana State University Coastal Studies Institute, Technical Report 76, 34p.